$LaFeO_3$ (1/1) superlattice. However, the magnetization value of 3 μ_B per site is too large to attribute to a ferrimagnetic order. The dependence of M on the magnetic field (hysteresis curve) of $LaCrO_3$-$LaFeO_3$ artificial superlattice (1/1 sequence) on substrate (111) is shown in Fig. 4. Hysteresis was observed in the M-*H* curves in the temperature region from 6 to 350 K. The M is saturated under the applied field above 5 kOe (Fig. 4B). In the enlarged hysteresis curve (Fig. 4A), the remnant M of the superlattices decreases with increasing temperature up to 375 K. Above a T_C of 375 K, it shows a paramagnetic character. These features are typical of FM materials. Our results provide further evidence that the FM spin order is realized in the artificial lattice with a one by one layer stacking combination.

REFERENCES AND NOTES

1. H. A. Kramers, *Physica* **1**, 182 (1934).
2. P. W. Anderson, *Phys. Rev.* **79**, 350 (1950).
3. J. B. Goodenough, *ibid.* **100**, 564 (1955).
4. J. Kanamori, *J. Phys. Chem. Solids* **10**, 87 (1959).
5. In the case of Ni^{2+} and Mn^{4+} or Co^{2+} and Mn^{4+}, FM ordering was reported in the bulk sample [G. Blasse, *J. Phys. Chem. Solids* **26**, 1969 (1965)].
6. A. Wold and W. Croft, *J. Phys. Chem.* **63**, 447 (1959).
7. A. Belayachi, M. Nogues, J.-L. Dormann, M. Taibi, *Eur. J. Solid State Inorg. Chem.* **33**, 1039 (1996).
8. K. P. Belov *et al.*, *Sov. Phys. Solid State* **14**, 813 (1972).
9. R. Aleorard, R. Pauthenet, J. P. Rebouillat, C. Veyret, *J. Appl. Phys.* **39**, 379 (1968).
10. W. C. Koehler, E. O. Wollan, M. K. Wilkinson, *Phys. Rev.* **118**, 58 (1960).
11. D. Treves, *J. Appl. Phys.* **36**, 1033 (1965).
12. T. Kawai, M. Kanai, H. Tabata, *Mater. Sci. Eng.* **41**, 123 (1996).
13. H. Tabata, T. Kawai, S. Kawai, *Phys. Rev. Lett.* **70**, 2633 (1993).
14. Targets of $LaCrO_3$ and $LaFeO_3$ were synthesized by mixing La_2O_3 with Cr_2O_3, and La_2O_3 with α-Fe_2O_3, respectively, at a molar ratio of 1:1 and sintering them at 1000°C. The films were formed at 580°C in an oxygen/ozone (8%) ambient pressure of 1 mtorr. The deposition rate was 10 Å/min. All magnetic measurements were performed with a SQUID magnetometer (Quantum design MPMS-5S).

13 January 1998; accepted 23 March 1998

Inducible Repair of Thymine Glycol Detected by an Ultrasensitive Assay for DNA Damage

X. Chris Le,* James Z. Xing, Jane Lee, Steven A. Leadon, Michael Weinfeld*

An ultrasensitive assay for measuring DNA base damage is described that couples immunochemical recognition with capillary electrophoresis and laser-induced fluorescence detection. The method provides a detection limit of 3×10^{-21} moles, an improvement of four to five orders of magnitude over current methods. Induction and repair of thymine glycols were studied in irradiated A549 cells (a human lung carcinoma cell line). Exposure of these cells to a low dose of radiation (0.25 Gray) 4 hours before a clinically relevant dose (2 Gray) enhanced removal of thymine glycols after the higher dose. These data provide evidence for an inducible repair response for radiation-induced damage to DNA bases.

DNA damage and its cellular repair are key determinants in the early stages of carcinogenesis, cancer therapy, and aging. As a result, many assays for DNA damage have been developed over the past 30 years; each has its advantages and disadvantages (*1*, *2*). Among the important criteria to consider when assessing the usefulness of an assay are its specificity, sensitivity, and simplicity. Measurement of oxidative DNA damage generated by ionizing radiation illustrates the relative importance of each of these criteria. Ionizing radiation produces a wide assortment of DNA lesions, including a large number of base modifications, strand breaks, and DNA-protein crosslinks (*3*). Because of their specificity, techniques such as gas chromatography–mass spectrometry, high-performance liquid chromatography with electrochemical and mass spectrometry detection, postlabeling, and immunoassays have proven extremely useful for analyzing modified bases (*4*). However, they currently lack the sensitivity required to monitor repair of the DNA of cells treated with clinically relevant doses of radiation—that is, ≤2 Gray (Gy). In addition, the first three methods involve a series of chemical derivatization or enzymatic hydrolysis and labeling steps, which means that great care must be taken to ensure that there is minimal introduction of oxidative DNA lesions by the procedure itself and that digestion and labeling reactions are optimized (*5*). On the other hand, electrophoretic approaches, such as pulsed-field gel electrophoresis and single-cell gel electrophoresis (the comet assay), have the capacity to detect damage at lower radiation doses but for the most part are restricted to measurement of strand breaks (*6*).

To monitor damage to DNA bases resulting from therapeutic doses of radiation, we have developed an assay that takes advantage of the high sensitivity (zeptomole, or 10^{-21} mol) afforded by capillary electrophoresis coupled with laser-induced fluorescence detection (*7*, *8*), combined with the specificity provided by monoclonal antibodies to a single lesion. Sample manipulation is limited to DNA extraction, incubation with antibodies, and capillary electrophoresis, thereby reducing potential artifacts caused by chemical or enzymatic DNA digestion. Notably, the technique requires only nanogram amounts of DNA.

To test the feasibility of the assay, we used mouse monoclonal antibodies to bromodeoxyuridine (BrdU) (*9*), because we could generate model DNA antigens containing a specified quantity of this modified base, and tetramethylrhodamine (TMR)-labeled secondary antibodies because of the convenient fluorescence wavelengths. To prepare the antigens, we cleaved pUC18 plasmid molecules with Sal I, filled in the overhanging termini by incorporating nucleotides including BrdU, and then ligated the plasmid molecules (*10*). Thus, two molecules of BrdU were incorporated per molecule of pUC18 [2690 base pairs (bp)]. Capillary electrophoresis separates the unbound secondary antibody (Fig. 1A, peak 1), the complex of secondary and primary antibody (Fig. 1B, peak 2), and the complex of antigen with the primary and secondary antibodies (Fig. 1C, peak 3). The signal in peak 3 (Fig. 1C) was produced by $\sim 3 \times 10^{-19}$ mol of BrdU.

We compared the signals produced by BrdU-containing plasmid DNA at a concentration of 0.05 μg/ml in the absence (Fig. 1D) or presence (Fig. 1E) of unmodified pUC18 DNA (450 μg/ml), which corresponds to a final ratio of 2 BrdU molecules per 2.42×10^7 bp. The large excess of undamaged DNA did not alter the signal in peak 3. Because the sample concentration of plasmid DNA antigen was 0.05 μg/ml and 1 nl was injected into the capillary, the signal in peak 3 represents $\sim 6 \times 10^{-20}$ mol of BrdU. The detection limit, based on a signal-to-noise ratio of 3, was 3×10^{-21}

X. C. Le and J. Z. Xing, Department of Public Health Sciences, Faculty of Medicine and Oral Health Sciences, University of Alberta, Edmonton, Alberta, T6G 2G3, Canada.
J. Lee and M. Weinfeld, Experimental Oncology, Cross Cancer Institute, Edmonton, Alberta, T6G 1Z2, Canada.
S. A. Leadon, Department of Radiation Oncology, University of North Carolina School of Medicine, Chapel Hill, NC 27599–7512, USA.
*To whom correspondence should be addressed. E-mail: xc.le@ualberta.ca and mweinfel@gpu.srv.ualberta.ca

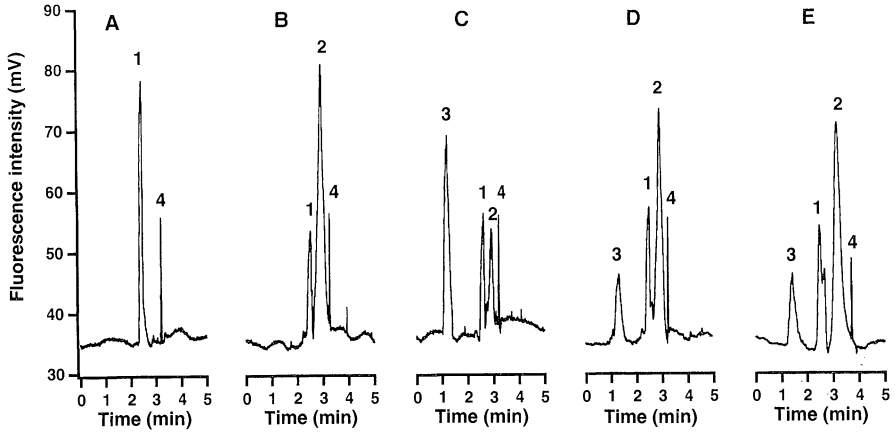

Fig. 1. Electropherograms showing separation of fluorescently labeled secondary antibody (peak 1), the complex of primary and secondary antibody (peak 2), and the complex of antigen with primary and secondary antibody (peak 3). (**A**) TMR-labeled anti-mouse secondary antibody (0.8 pg; 1 nl of 0.8-μg/ml solution) (Calbiochem, La Jolla, CA) in 10 mM tris-HCl buffer (pH 7.3). (**B**) A mixture of (A) and 0.4 pg of mouse monoclonal antibody to BrdU (*9*). (**C**) A mixture of (B) and 0.25 pg of pUC18 plasmid DNA containing BrdU. (**D**) A mixture containing 0.8 pg of TMR-labeled anti-mouse secondary antibody, 0.4 pg of mouse monoclonal antibody to BrdU, and 0.05 pg of pUC18 plasmid DNA containing BrdU. (**E**) A mixture of (D) and 450 pg of unmodified pUC18 DNA. Peak 4 is due to the free TMR in the secondary antibody reagent solution. The presence of this fluorescent compound in all assays makes it a good internal standard to correct for changes in instrument sensitivity. The electropherograms were obtained with a capillary electrophoresis system built in the laboratory with laser-induced fluorescence detection, similar to that described previously (*8*), except without the use of a sheath flow cuvette. Separation was carried out in a 42-cm-long, 20-μm inner diameter, and 145-μm outer diameter fused silica capillary at an electric field of 400 V/cm. The detection window was 35 cm from the injection end of the capillary. The separation buffer (pH 10.5) contained 20 mM borate and 10 mM tris-HCl. Electrokinetically injected sample volume was ~1 nl.

mol, which represents an improvement of 4 to 5 orders of magnitude over currently available assays for DNA base damage.

We next performed experiments with antibodies to 5,6-dihydroxy-5,6-dihydrothymine [thymine glycol (Tg)] to determine a detection limit in terms of radiation dose and to compare the yield of Tg induced in cellular DNA versus naked DNA. The primary antibodies were mouse monoclonal antibodies against OsO_4-treated polydeoxythymidine (*11*), which are highly specific for Tg against a background of unmodified thymine in DNA. We used calibration based on BrdU DNA standards to quantify Tg from measured fluorescence intensities (*12*). Using the BrdU calibration, we determined that irradiation of A549 cells with 1 Gy yields 0.9 ± 0.2 Tg per 10^7 DNA bases. This agrees with a previous report (*13*) showing that irradiation of human fibroblasts with 10 Gy of x-rays produces 0.95 ± 0.12 Tg per 10^6 DNA bases. A typical series of electropherograms obtained with DNA extracted from irradiated human lung carcinoma cells (A549 cell line) is shown in Fig. 2. The signal with unirradiated DNA was so low that, despite the use of a fairly protracted extraction protocol (*14*), it was possible to detect Tg at doses below 0.05 Gy. The Tg signal detected after 0.05-Gy irradiation corresponds to 4.3 Tg per 10^9 bases. The detection limit, based on a signal-to-noise ratio of 3, was ~1 Tg per 10^9 bases.

We compared the dose response for the yield of Tg produced by up to 1-Gy irradiation for naked DNA and cellular DNA (Fig. 3). For naked DNA, either isolated from A549 cells or from a commercially available preparation of calf thymus DNA, there was a linear response up to 1 Gy, and thereafter saturation was observed unless the DNA was diluted or the amounts of secondary and primary antibodies were in-

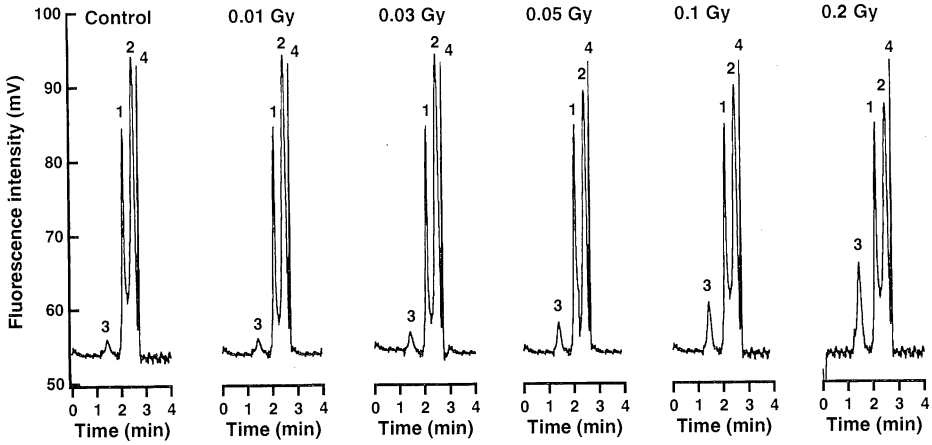

Fig. 2. Representative electropherograms showing the yield of Tg in A549 human lung carcinoma cells irradiated with increasing doses (0.01 to 0.2 Gy) from a ^{137}Cs γ-ray source. A sample of the extracted cellular DNA was incubated with the TMR-labeled anti-mouse secondary monoclonal antibody in 10 mM tris-HCl (pH 7.3) for 5 min at room temperature (20° to 25°C) and further incubated with a primary mouse monoclonal antibody to Tg (*11*) under the same conditions for another 20 min. A 1-nl sample of the mixture containing 25 μg of DNA per milliliter was injected into the capillary for the assay.

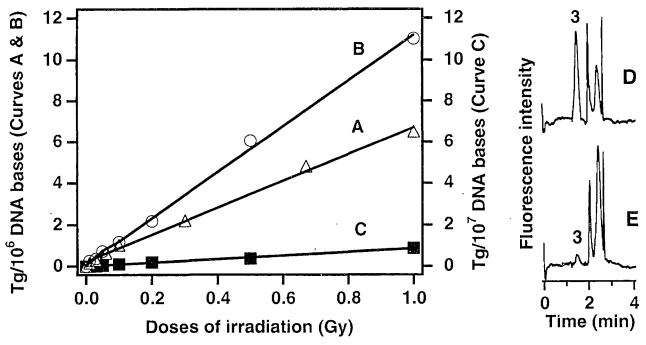

Fig. 3. Comparison of the yield of Tg generated by irradiation (0.01 to 1 Gy) of calf thymus DNA (**A**), naked DNA extracted from A549 cells (**B**), and A549 cells (**C**). Left vertical axis is for (A) and (B), and right axis is for (C). Calf thymus DNA (Sigma) in aqueous solution was directly irradiated with the specified doses and the Tg was then assayed. A549 cells and the naked DNA extracted from A549 cells were separately irradiated with the specified doses and the Tg was then assayed. The ratios of the slopes of the linear curves are 72 (ratio of A to C) and 122 (ratio of B to C), respectively, which represents the protection factor afforded by the cells to the DNA. Comparison of irradiated (5 Gy) calf thymus DNA before (**D**) and after (**E**) treatment with *E. coli* endonuclease III (6 ng of enzyme per microgram of DNA) confirms that peak 3 is due to Tg.

creased. We observed linearity with DNA from irradiated A549 cells up to and including 5 Gy, the highest dose examined. The slopes of the three curves indicate that 1 Gy induces 0.9 Tg per 10^7 bases in cellular DNA, 11 Tg per 10^6 bases in naked DNA extracted from A549 cells, and 6.5 Tg per 10^6 bases in calf thymus DNA in dilute aqueous solution. Thus, the cell affords about 70- to 120-fold protection to its DNA, which is consistent with previous data (*10, 15*).

We obtained confirmation that the assay was measuring Tg by incubating irradiated DNA (Fig. 3D) with *Escherichia coli* endonuclease III, which resulted in almost complete loss of peak 3 (Fig. 3E).

Eukaryotic cells are known to have an inducible or adaptive response that enhances their radioresistance after a low priming dose of radiation (*16*). There is also evidence suggesting that a substantial component of radioresistance shown by tumor cells may be inducible rather than constitutive (*17, 18*). Because hydrogen peroxide, another DNA damaging agent, similarly enhances resistance to subsequent x-irradiation (*19*), and because the adaptive response appears to be inhibited by agents that inhibit DNA repair and protein synthesis (*18–20*), enhanced DNA repair, especially that of double-strand breaks (*21*), has been implicated as a mechanism underlying the inducible response. However, this phenomenon has not been examined directly by monitoring the repair of DNA base lesions.

Toward this end, we irradiated A549 cells with either a typical clinical dose of 2 Gy or with 0.25 Gy 4 hours before the 2-Gy irradiation. We then monitored removal of Tg over a 24-hour period. Without prior low-dose irradiation there was a reasonably rapid removal of up to 80% of Tg over the first 4 hours (Fig. 4), although there was a perceptible lag in repair over the first 30 min. Prior low-dose irradiation did not alter the initial induction of Tg after the 2-Gy dose, but it clearly enhanced the initial rate of lesion removal, reducing the time for 50% removal from ~100 to ~50 min. Much of this appears attributable to the absence of an early lag period. Thus, our experiments suggest that there is an inducible repair response for radiation-induced DNA base damage.

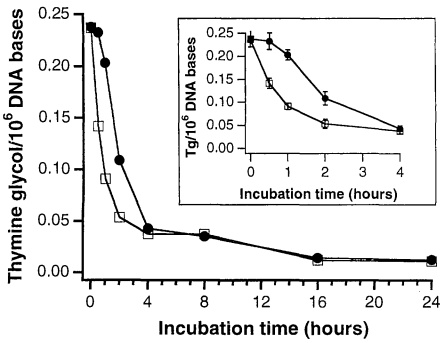

Fig. 4. Comparison of removal of Tg by A549 cells with and without a priming dose of radiation. We irradiated A549 cells with 2 Gy and then incubated them at 37°C for the specified time before the DNA was extracted (●), or we gave a priming dose of 0.25 Gy and incubated the cells at 37°C for 4 hours before the 2-Gy dose and then allowed the cells to carry out repair (□). (Inset) An expanded region between 0 and 4 hours. Error bars represent one standard deviation from six replicate assays of duplicate sets of cells.

In human cells, the predominant mode of repair for Tg is considered to be the base excision repair pathway, and hNth, the human homolog of *E. coli* endonuclease III, is the major glycosylase that removes the modified base from DNA (*22*). However, Tg also appears to be recognized in vitro by enzymes of the nucleotide excision repair pathway (*23*), and there is strong evidence that repair in actively transcribed genes may be coupled to transcription (*13*). It remains to be seen whether the observed inducible response reflects increased expression of hNth activity or an alternative mechanism possibly coupled to nucleotide excision repair or one or more cell-cycle checkpoints (*24*).

The ultrasensitive assay described here is not limited to detection of Tg but conceivably could be extended to other base lesions, provided that appropriate affinity probes are available. In addition to potential clinical application, this assay could allow DNA damage to be a direct biomarker for human exposures to carcinogens. Rather than the current reliance on extrapolation of orders of magnitude from high-dose bioassays with rodents (*25*), a sufficiently sensitive measure of DNA damage could allow for a more realistic assessment of environmental risk. With further automation, our assay could monitor specific DNA damage from environmental and occupational exposures in large cohorts.

REFERENCES AND NOTES

1. E. C. Friedberg and P. C. Hanawalt, Eds., *DNA Repair. A Laboratory Manual of Research Procedures* (Dekker, New York, 1988).
2. G. P. Pfeifer, Ed., *Technologies for Detection of DNA Damage and Mutations* (Plenum Press, New York, 1996).
3. C. von Sonntag, *The Chemical Basis of Radiation Biology* (Taylor and Francis, London, 1987).
4. M. Dizdaroglu, *Methods Enzymol.* **234**, 3 (1994); H. Kaur and B. Halliwell, *Biochem. J.* **318**, 21 (1996); M. Weinfeld and K.-J. Soderlind, *Biochemistry* **30**, 1091 (1991); R. J. Melamede, Y. W. Kow, I. A. Bespalov, S. S. Wallace, in (*2*), pp. 103–115.
5. J.-L. Ravanat, R. J. Turesky, E. Gremaud, L. J. Trudel, R. H. Stadler, *Chem. Res. Toxicol.* **8**, 1039 (1995); T. Douki, T. Delatour, F. Bianchini, J. Cadet, *Carcinogenesis* **17**, 347 (1996); K. B. Beckman and B. N. Ames, *J. Biol. Chem.* **272**, 19633 (1997); K. Hemminki *et al.*, *IARC* (*Int. Agency Res. Cancer*) Sci. Publ. **124**, 51 (1993); M. Weinfeld, M. Liuzzi, G. D. D. Jones, in (*2*), pp. 63–71.
6. J. A. Longo, B. Nevaldine, S. L. Longo, J. A. Winfield, P. J. Hahn, *Radiat. Res.* **147**, 35 (1997); D. W. Fairbairn, P. L. Olive, K. L. O'Neill, *Mutat. Res.* **339**, 37 (1995).
7. Y.-F. Cheng and N. J. Dovichi, *Science* **242**, 562 (1988); B. B. Haab and R. A. Mathies, *Anal. Chem.* **67**, 3253 (1995); S. Nie, D. T. Chiu, R. N. Zare, *Science* **266**, 1018 (1994).
8. X. C. Le *et al.*, *J. Chromatogr. A* **716**, 215 (1995).
9. S. A. Leadon, *Nucleic Acids Res.* **14**, 8979 (1986).
10. M. A. Chaudhry and M. Weinfeld, *J. Mol. Biol.* **249**, 914 (1995).
11. S. A. Leadon and P. C. Hanawalt, *Mutat. Res.* **112**, 191 (1983).
12. To obtain optimum conditions, we varied the ratios of the immunoreagents and the antigen (BrdU or Tg). In particular, we used an excess of fluorescently labeled secondary antibody to complex with all available primary antibody; similarly, we maintained an excess of both secondary and primary antibodies over the amount of antigen. Thus, the complex of antigen with the primary antibody was completely labeled with the secondary antibody and was detected by laser-induced fluorescence. This important consideration has been demonstrated in all electropherograms, which always show the presence of peak 1 (excess unbound secondary antibody) and peak 2 (complex of primary and secondary antibodies). Peak 4, which is also present in all electropherograms, arises from the free fluorophore TMR, an impurity present in the secondary antibody reagent. We used peak 4 as an internal standard to correct for changes of instrument sensitivity. Because the primary antibody is saturated with the secondary antibody and because the fluorescence from the same secondary antibody is measured, the relative fluorescence intensity from 1 mol of Tg should be equal to that from 1 mol of BrdU. Thus, we quantified Tg from measured fluorescence intensities by using calibration against BrdU DNA standards.
13. P. K. Cooper, T. Nouspikel, S. G. Clarkson, S. A. Leadon, *Science* **275**, 990 (1997).
14. We cultured cells in Dulbecco's modified Eagle's medium/F12 medium supplemented with 10% fetal bovine serum. We discarded the medium immediately before irradiation, rinsed the cells, and then held them in ice-cold phosphate-buffered saline during irradiation. We irradiated the cells in a Shepherd Mark I-68A ^{137}Cs irradiator (J. L. Shepherd and Associates, San Fernando, CA). In all cases, exposure to the desired dose of radiation was kept to less than 3 min. Immediately after irradiation (or a period of repair in medium at 37°C), we lysed the cells by incubating them for 30 min at 60°C in NET buffer [50 mM tris-HCl (pH 9.0), 150 mM NaCl, 15 mM EDTA] containing 0.02% SDS and proteinase K at 20 mg/ml. We extracted and precipitated nucleic acids and removed RNA, after resuspension of the samples in 1% NET buffer, by adding ribonuclease (RNase) A (10 mg/ml) and RNase T1 (10 units/ml) and incubating at 37°C for 30 min. We again extracted and precipitated nucleic acids and dissolved the DNA in 10 mM tris-HCl (pH 7.6) and 1 mM EDTA. We used ultraviolet spectrometry to determine DNA concentrations.
15. M. Ljungman, *Radiat. Res.* **126**, 58 (1991); M. Ljungman, S. Nyberg, J. Nygren, M. Eriksson, G. Ahnstrom, *ibid.* **127**, 171 (1991).
16. G. Olivieri, J. Bodycote, S. Wolff, *Science* **223**, 594 (1984); S. Wolff, V. Afzal, J. K. Wiencke, G. Olivieri, A. Michaeli, *Int. J. Radiat. Biol.* **53**, 39 (1988); B. Marples and K. A. Skov, *Radiat. Res.* **146**, 382 (1996).
17. M. C. Joiner *et al.*, *Mutat. Res.* **358**, 171 (1996); P. Lambin, E. P. Malaise, M. C. Joiner, *Int. J. Radiat. Biol.* **69**, 279 (1996).
18. B. Marples, P. Lambin, K. A. Skov, M. C. Joiner, *Int. J. Radiat. Biol.* **71**, 721 (1997).
19. B. Marples and M. C. Joiner, *Radiat. Res.* **141**, 160 (1995).
20. J. H. Youngblom, J. K. Wienke, S. Wolff, *Mutat. Res.*

227, 257 (1989); J. Seong, C. O. Suh, G. E. Kim, *Int. J. Radiat. Oncol. Biol. Phys.* **33**, 869 (1995).
21. T. Ikushima, H. Aritomi, J. Morisita, *Mutat. Res.* **358**, 193 (1996); S. Lehnert and T. Y.-K. Chow, *Radiat. Environ. Biophys.* **36**, 67 (1997).
22. R. Aspinwall *et al.*, *Proc. Natl. Acad. Sci. U.S.A.* **94**, 109 (1997); T. P. Hilbert, W. Chaung, R. J. Boorstein, R. P. Cunningham, G. W. Teebor, *J. Biol. Chem.* **272**, 6733 (1997).
23. Y. W. Kow, S. S. Wallace, B. Van Houten, *Mutat. Res.* **235**, 147 (1990); J. T. Reardon, T. Bessho, H. C. Kung, P. H. Bolton, A. Sancar, *Proc. Natl. Acad. Sci. U.S.A.* **94**, 9463 (1997).
24. D. A. Boothman, M. Meyers, E. Odegaard, M. Wang, *Mutat. Res.* **358**, 143 (1996).
25. P. H. Abelson, *Science* **265**, 1507 (1994).
26. We thank N. Dovichi, S. Hrudey, and T. Lindahl for reviewing the manuscript and M. Ma, L. Ye, W. Ansbacher, and S. Kuny for technical assistance. Supported by grants from the Natural Sciences and Engineering Research Council of Canada, the National Cancer Institute of Canada, the Alberta Heritage Foundation for Medical Research through the Eco-Research Chair, the Alberta Cancer Board, and NIH (CA40453 and CA62059).

21 January 1998; accepted 3 April 1998

Inhibitory Function of $p21^{Cip1/WAF1}$ in Differentiation of Primary Mouse Keratinocytes Independent of Cell Cycle Control

Ferdinando Di Cunto, Gabrielle Topley, Enzo Calautti, Jimmy Hsiao, Lydia Ong, Prem K. Seth, G. Paolo Dotto*

The cyclin-dependent kinase inhibitor $p21^{Cip1/WAF1}$ has been implicated as an inducer of differentiation. However, although expression of p21 is increased in postmitotic cells immediately adjacent to the proliferative compartment, its expression is decreased in cells further along the differentiation program. Expression of the p21 protein was decreased in terminally differentiated primary keratinocytes of mice, and this occurred by a proteasome-dependent pathway. Forced expression of p21 in these cells inhibited the expression of markers of terminal differentiation at both the protein and messenger RNA levels. These inhibitory effects on differentiation were not observed with a carboxyl-terminal truncation mutant or with the unrelated cyclin-dependent kinase inhibitor $p16^{INK4a}$, although all these molecules exerted similar inhibition of cell growth. These findings reveal an inhibitory role of p21 in the late stages of differentiation that does not result from the effects of p21 on the cell cycle.

A precise coupling between cell growth and differentiation is required during embryonic development and in self-renewing tissues of the adult. The cyclin-dependent kinase (CDK) inhibitor $p21^{Cip1/WAF1}$ inhibits cell growth and, in some circumstances, promotes differentiation (*1*). However, in many tissues, expression of p21 in vivo correlates with the onset but not necessarily the establishment of the terminally differentiated phenotype (*2*, *3*). For instance, in the intestine, p21 expression is induced in postmitotic cells adjacent to the proliferative compartments, but is down-modulated at later stages of differentiation. Similarly, in hair follicles of the skin, p21 is highly expressed in a narrow zone of postmitotic keratinocytes next to the proliferating cells of the lower bulb, whereas little or no p21 is expressed in the differentiated keratinocytes of the upper region (*2*).

We examined the functional meaning of decreased p21 expression at late stages of differentiation in mouse keratinocytes. Addition of calcium (1.2 to 2 mM) to cultures of primary keratinocytes triggers a terminal differentiation program that includes early structural changes, such as desmosome formation and reorganization of keratin cables, as well as later events, such as growth arrest and expression of markers of the upper differentiated layers of the epidermis (*4*). Increased expression of p21 occurs 4 to 8 hours after exposure to calcium, along with inhibition of CDK and block of the cell cycle at the G_1 phase (*5*, *6*). After 24 hours, despite a sustained increase in p21 mRNA expression, the p21 protein returns to basal amounts or less (*6*).

Primary keratinocytes cultured in low-calcium medium (0.05 mM calcium) consist of two populations: continuously proliferating attached cells and terminally differentiated detached cells (*7*). The p21 protein was present in the attached keratinocytes but was almost undetectable in the detached population (Fig. 1A). No change was detected in the amount of the closely related CDK inhibitor p27, nor of p53 or cyclin A, the amount of which decreases after detachment in other cell types (*8*) (Fig. 1A). The amounts of p21 mRNA in the detached and attached populations were similar (Fig. 1B). Human and mouse keratinocytes can be induced to terminally differentiate when they are artificially brought into suspension by trypsinization (*7*, *9*). Amounts of the p21 protein were decreased even under these conditions (Fig. 1C), with a time course similar to that of expression of terminal differentiation markers (*10*). Expression of p21 was similarly reduced in the detached versus attached populations of keratinocytes derived from p53 null mice (Fig. 1D).

The p21 protein is a substrate for ubiquitination and proteasome-dependent degradation (*11*). Primary keratinocytes were treated for 24 hours with two chemically unrelated proteasome inhibitors, *N*-acetyl-leucinyl-leucinyl-norleucinal (LLnL) and lactacystin (*12*), or with an inhibitor of cysteine proteinases devoid of any inhibitory activity toward the proteasome, L-*trans*-epoxysuccinic acid (E64) (*13*). The latter compound had no effect on the amount of p21 in either attached or spontaneously detached keratinocytes (Fig. 1E). By contrast, the amount of p21 was increased in attached keratinocytes from cultures treated with either LLnL or lactacystin, at concentrations as low as 3 μM. Similar large amounts of p21 protein were also present in the corresponding detached populations. Moreover, in extracts of keratinocytes treated with proteasome inhibitors, but not in those with E64, antibodies to p21 (anti-p21) recognized specific bands of larger molecular size that are likely to correspond to ubiquitinated forms of p21 (Fig. 1E). Treatment with proteasome inhibitors led to no increase in expression of p21 mRNA, but rather a slight decrease (Fig. 1F). Proteasome inhibitors also counteracted the decrease in the amount of p21 protein that occurred when keratinocytes were artificially brought into suspension by trypsinization (*10*). Thus, a specific proteasome-mediated pathway contributes to decreased expression of p21 in differentiated keratinocytes.

To assess the biological meaning of decreased p21 expression in differentiation, we infected primary keratinocytes with a control adenovirus expressing a bacterial β-galactosidase gene (Ad-lac z) and an adenovirus expressing full-length human p21 (Ad-p21) (*14*). Infection of cells with the Ad-p21 virus caused inhibition of DNA synthesis by 24 hours after infection; no

F. Di Cunto, Cutaneous Biology Research Center, Massachusetts General Hospital and Harvard Medical School, 13th Street, Charlestown, MA 02129, USA, and Department of Biology, Genetics and Medical Chemistry, University of Torino, Via Santena 5 bis, Torino, Italy.
G. Topley, E. Calautti, J. Hsiao, L. Ong, G. P. Dotto, Cutaneous Biology Research Center, Massachusetts General Hospital and Harvard Medical School, 13th Street, Charlestown, MA 02129, USA.
P. K. Seth, Breast Cancer Section, Medicine Branch, National Cancer Institute, Building 10, Bethesda, MD 20892, USA.
*To whom correspondence should be addressed. E-mail: Paolo_Dotto@cbrc.mgh.harvard.edu